

pubs.acs.org/JPCL Letter

Nonorthogonal Active Space Decomposition of Wave Functions with Multiple Correlation Mechanisms

Emily M. Kempfer-Robertson, Andrew D. Mahler, Meagan N. Haase, Piper Roe, and Lee M. Thompson*



Cite This: J. Phys. Chem. Lett. 2022, 13, 12041-12048



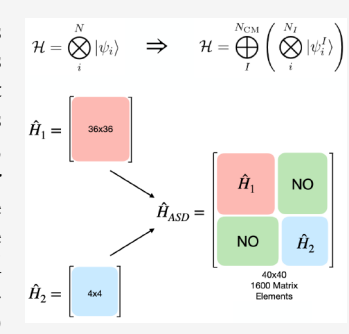
ACCESS I

III Metrics & More

Article Recommendations

SI Supporting Information

ABSTRACT: The nonorthogonal active space decomposition (NO-ASD) methodology is proposed for describing systems containing multiple correlation mechanisms. NO-ASD partitions the wave function by a correlation mechanism, such that the interactions between different correlation mechanisms are treated with an effective Hamiltonian approach, while interactions between correlated orbitals in the same correlation mechanism are treated explicitly. As a result, the determinant expansion scales polynomially with the number of correlation mechanisms rather than exponentially, which significantly reduces the factorial scaling associated with the size of the correlated orbital space. Despite the nonorthogonal framework of NO-ASD, the approach can take advantage of computational efficient matrix element evaluation when performing nonorthogonal coupling of orthogonal determinant expansions. In this work, we introduce and examine the NO-ASD approach in comparison to complete active space methods to establish how the NO-ASD approach reduces the problem dimensionality and the extent to which it affects the amount of



correlation energy recovered. Calculations are performed on ozone, nickel-acetylene, and isomers of μ -oxo dicopper ammonia.

S trong correlation, otherwise known as a non-dynamical or static correlation, arises when an electronic state does not have a well-defined set of occupied orbitals. As a result, the wave function is an entangled superposition of electron configurations, with permanent interactions between electrons at fractionally occupied sites that occur over long distances. A challenge in the development of electronic structure methods that are able to account for strong correlation is the identification of the relevant correlated orbital space $\{|\psi_i\rangle\}$. Once the correct orbital subspace has been identified, accounting for the interactions between all N sites can be performed numerically by solving for the wave function in the Hilbert space $\mathcal H$ constructed as the tensor product of $\{|\psi_i\rangle\}$

$$\mathcal{H} = \bigotimes_{i}^{N} |\psi_{i}\rangle \tag{1}$$

which leads to O(N!) scaling in the dimensionality of \mathcal{H} . As a result of the factorial scaling with the number of strongly correlated sites, it is desirable to minimize the value of N. Through occupied—occupied (oo) and virtual—virtual (vv) orbital transformations, it is possible to minimize the expansion in eq 1 by "concentrating" the strong correlation in as small of a subset of orbitals as possible. Löwdin was the first to recognize that the smallest possible orbital subset that recovers the strong correlation is the fractionally occupied natural orbitals (NOs) of the full configuration interaction (FCI) density. To establish the correct subset of orbitals without resorting to their explicit calculation, Pulay and co-workers developed the unrestricted natural orbital (UNO) approach, in which the fractionally occupied NOs of symmetry-broken self-consistent field density matrices are used. While it is known

that symmetry breaking in mean-field wave functions is a marker of strong correlation, only recently has it been possible to demonstrate the validity of the UNO approach by comparison to the very large active spaces afforded by the density matrix renormalization group (DMRG).⁵

Despite the success of the UNO approach, difficulties are encountered in the presence of multiple correlation mechanisms (MCMs). MCMs can be defined as situations in which one or more strongly correlated occupied orbitals has multiple correlation partners.^{4,5} An alternative definition of MCMs is that all possible reference self-consistent field (SCF) solutions have fractionally occupied NOs that describe only a subspace of the FCI NOs, such that any determinant expansion in one of the SCF solution NOs is unable to span the strongly correlated subspace of the FCI Hilbert space. As a result, strong correlations in wave functions with MCMs cannot be treated by projection-after-variation methods or standard UNO approaches, because SCF symmetry breaking cannot fully reveal the set of strongly correlated orbitals. Early in the development of the UNO method, it was noted that multiple correlation mechanisms are signaled by the presence of several nearly degenerate SCF solutions. To resolve this issue in the UNO framework, the NOs of the averaged density matrices

Received: November 4, 2022 Accepted: December 16, 2022



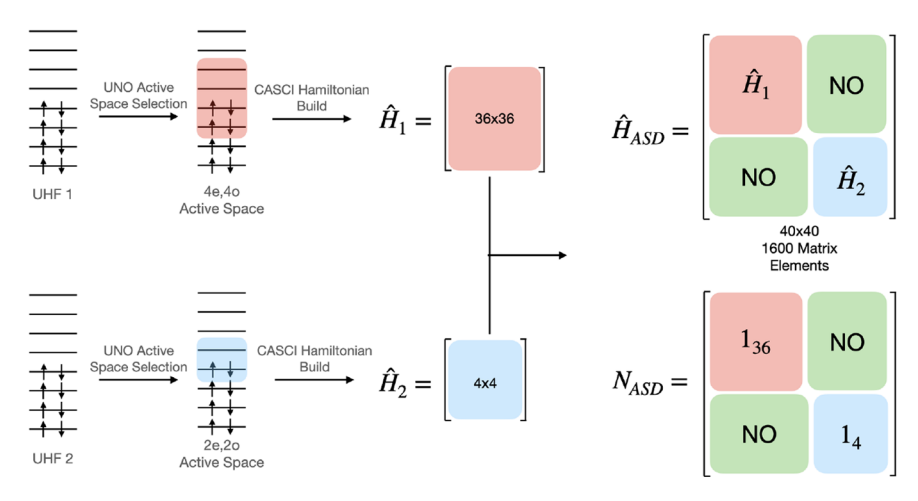


Figure 1. Schematic for formation of the nonorthogonal active space decomposition scheme Hamiltonian \hat{H}_{ASD} and overlap N_{ASD} indicating diagonal block orthogonal and off-diagonal block nonorthogonal components.

were used.⁵ While the averaged-density UNO method enables the identification of the minimum required subset of orbitals to describe the strong correlation, the approach still has factorial scaling in the number of correlated orbitals according to eq 1. A question that arises is whether the partitioning of the wave function indicated by different SCF solutions can be utilized in a different way that avoids the factorial scaling in the correlated orbital space. In other words, can interactions between correlated mechanisms be treated differently to interactions within correlation mechanisms in such a way that the method scales polynomially with the number of correlation mechanisms?

In this paper, we propose to couple together separate UNO expansions through nonorthogonal Hamiltonian blocks, which can dramatically reduce the scaling of the required wave function expansion. The proposed nonorthogonal active space decomposition (NO-ASD) approach is related to several other methods, including active space decomposition, blocklocalized wave function, molecular orbital-valence bond theory, nonorthogonal configuration interaction with multiconfigurational fragment wave functions representing the diabatic states (NOCI-F), and constrained density functional theory configuration interaction (CDFTCI), ¹⁰ in that fragment wave functions are constructed and used to partition a configuration interaction (CI) active space. However, the proposed approach differs as the fragments are defined entirely self-consistently rather than using arbitrary constraints or spatial partitioning of the molecule. Instead of solving for the wave function in the Hilbert space defined by eq 1, the wave function is determined in the Hilbert space formed from the direct sum of the separate UNO expansions on each SCF solution

$$\mathcal{H} = \bigoplus_{I}^{N_{\text{CM}}} \left(\bigotimes_{i}^{N_{I}} |^{I} \psi_{i} \rangle \right) \tag{2}$$

where the index I indicates the correlation mechanism. As a result, the formulation in eq 2 properly treats entanglement between orbitals within each correlation mechanism but gives an unentangled superposition of different correlation mechanisms. However, because each correlation mechanism is generally constructed from a set of orbitals that are nonorthogonal to the set of orbitals in other correlation mechanisms, orbitals in each correlation mechanism can be

expressed as disconnected single excitation cluster operators acting to infinite order in the basis of a common set of orthogonal orbitals.¹¹ As a result, entanglement between orbitals in different correlation mechanisms that is not formally included in the determinant expansion is implicitly wrapped in. Therefore, NO-ASD recovers entanglement through an effective Hamiltonian approach, in contrast to explicit tensor decomposition.¹² It is important to note that the full tensor product in eq 2 may produce larger determinant expansions than necessary, and these additional determinants may in fact lead to greater errors. As demonstrated in the context of the multistate density functional theory (DFT), a minimal active space with half projection of open-shell determinants is all that should be required. 13-15 However, here, we opt for complete active space (CAS) expansions to ensure the connection with the active space decomposition philosophy embodied by eq 2 and to enable direct comparison to CAS wave functions.

The workflow of performing the NO-ASD scheme is as follows: First, the relevant set of SCF solutions must be identified. In this regard, UNO and NO-ASD approaches are equivalent in the extent to which they are black boxes. More generally, understanding and identifying relevant SCF solutions is still a challenge and an active area of research, 16,17 with several local SCF optimization techniques and global searching algorithms having been developed in recent years. 18-24 Typically, the nearly degenerate low-energy SCF solutions are the relevant set, which simplifies solution identification. Subsequently, from the identified SCF solutions, a determinant CAS expansion is constructed in the fractionally occupied set of NOs for each SCF solution. The resulting orthogonal determinant expansions are then coupled using nonorthogonal configuration interaction (NOCI) (Figure 1). In this work, we investigate the NO-ASD-CI method, where the molecular orbitals are fixed and the CI coefficients are linearly optimized. Nonorthogonal Hamiltonian matrix elements can be computed according to the generalized Slater-Condon rules, 25,26 and the energy can be determined by solving the generalized eigenvalue problem

$$HD = NDE \tag{3}$$

where **H** is the Hamiltonian matrix, **N** is the Slater determinant or configuration state function overlap matrix, and **D** and **E** are

the eigenvectors and eigenvalues, respectively. The NO-ASD wave function for state A is then written as

$$\begin{split} \Psi_{A} &= \sum_{I}^{N_{\text{CM}}} \left(^{IA}D_{0} |^{I}\Psi_{0}\rangle + \sum_{ux} {}^{IA}D_{ux} |^{I}\Psi_{u}^{x}\rangle + \sum_{uvxy} {}^{IA}D_{uvxy} |^{I}\Psi_{xy}^{uv}\rangle \right. \\ &\left. + \sum_{uvwxyz} {}^{IA}D_{uvxy} |^{I}\Psi_{uvw}^{xyz}\rangle + \ldots \right) \end{split} \tag{4}$$

where u, v, x, \ldots indicate active space orbitals that are occupied in the reference determinant $I^I\Psi_0\rangle$, x, y, z, \ldots are active space orbitals that are virtual in the reference determinant, and $\{D\}$ values are the CI coefficients. Evaluation in the atomic orbital (AO) basis yields a maximum $O(N_{\rm basis}^4)$ scaling for each matrix element, although in practice diagonal blocks can be computed using standard orthogonal CI techniques, and matrix elements in off-diagonal nonorthogonal blocks only need to be evaluated if the number of occupied orbitals with zero overlap between determinants is less than or equal to 2, where the overlap can be evaluated at $O(N_{\rm elec}^3)$ cost.

Given the nature of the determinant expansion in NO-ASD, a more effective algorithm is to evaluate matrix elements in the nonorthogonal blocks in the molecular orbital (MO) basis, owing to the fact that only a single integral transformation at $O(N_{\rm basis}^5)$ cost is required for each pair of correlation mechanisms included in the calculation. The subsequent contractions required to compute matrix elements are then reduced to $O(N_{\rm occ}^4)$. The rules for matrix elements in the MO basis are as follows:

$${}^{IJ}N\left(\sum_{ij}{}^{IJ}h_{ij}{}^{IJ}M_{ji}^{-1} + \frac{1}{2} \qquad \text{for dim}(\ker({}^{IJ}\mathbf{M})) \\ = 0$$

$$\sum_{ijkl}{}^{IJ}\langle ij||kl\rangle^{IJ}M_{ki}^{-1IJ}M_{lj}^{-1}\right) \qquad = 0$$

$${}^{IJ}\tilde{N}\left(\sum_{ij}{}^{IJ}h_{ij}U_{ip}V_{jp} \qquad \text{for dim}(\ker({}^{IJ}\mathbf{M})) \\ = 1$$

$$+\sum_{ijkl}{}^{IJ}\langle ij||kl\rangle U_{jp}V_{lp}{}^{IJ}M_{ki}^{+}\right) \qquad = 1$$

$${}^{IJ}\tilde{N}\sum_{ijkl}{}^{IJ}\langle ij||kl\rangle U_{iq}U_{jp}V_{kq}V_{lp} \qquad \text{for dim}(\ker({}^{IJ}\mathbf{M})) \\ = 2$$

$$0 \qquad \qquad \text{for dim}(\ker({}^{IJ}\mathbf{M})) \\ > 2 \qquad (5)$$

where i, j, k, ... are occupied orbital indices, p, q, r, ... are indices of biorthogonalized orbitals with zero overlap between determinants I and J, $\dim(\ker(^{IJ}\mathbf{M}))$ indicates the size of the null space (number of biorthogonalized orbitals with zero overlap) of the oo overlap matrix $^{IJ}\mathbf{M}$, which is computed using the occupied molecular orbital coefficients \mathbf{C}_{occ} and atomic orbital overlap matrix \mathbf{S} as

$${}^{IJ}\mathbf{M} = {}^{I}\mathbf{C}_{\text{occ}}^{\dagger} \mathbf{S}^{J} \mathbf{C}_{\text{occ}}$$
 (6)

 $^{IJ}\tilde{\mathbf{N}}$ is the reduced overlap, computed from the pseudodeterminant of $^{IJ}\mathbf{M}$, $^{IJ}\mathbf{M}^+$ indicates the Moore–Penrose pseudoinverse of $^{IJ}\mathbf{M}$, h_{ij} and $\langle ij||kl\rangle$ are one-electron and antisymmetrized two-electron integrals in the MO basis, respectively, and the matrices \mathbf{U} and \mathbf{V} are computed from singular value decomposition of $^{IJ}\mathbf{M}$

$$^{IJ}\mathbf{M} = \mathbf{U}^{IJ}\boldsymbol{\sigma}\mathbf{V}^{\dagger} \tag{7}$$

Very recent work by Burton invoking a nonorthogonal generalized Wick's theorem has been shown to further reduce the scaling to be independent of the system size entirely. 27,28 Although the generalized Wick's theorem approach requires storage of a large number of sets of transformed two-electron integrals and, therefore, has a greater memory cost than the MO basis calculation presented, the reduction in the cost of subsequently evaluating each matrix element from $O(N_{\rm occ}^4)$ to O(1) has the potential to significantly extend the size of NO-ASD determinant expansions.

A well-known issue with the selection of the active space based on occupation number thresholds is the presence of discontinuities in the potential energy surface (PES). In fact, these discontinuities are present in all multiconfigurational calculations.^{3,29} To minimize threshold-based discontinuities, the same approach could be used in NO-ASD as in UNO, in which natural orbitals are computed at the geometry that gives the largest active space and then the identified active space used across the entire PES. Alternatively, natural orbitals of half-projected determinants may also ameliorate discontinuities.30 However, natural orbitals of individual symmetrybroken SCF solutions typically display greater fractional occupation (lower levels of intermediate correlation) than the averaged density, and therefore, NO-ASD is less likely to suffer from the choice of threshold than averaged density UNO methods (section S3 of the Supporting Information). A related issue that leads to discontinuities is the disappearance of SCF solutions as the geometry changes, which is fundamentally related to changes in the correlation mechanisms that are acting at a given geometry. Because the relevant SCF solutions are the same in UNO and NO-ASD, both methods are likely to be affected by disappearing solutions to the same extent. However, using holomorphic solutions^{31,32} or coupleddeterminant orbital reoptimization³³ may provide a solution to resolve the effect of vanishing solutions.

In the remainder of this work, NO-ASD results are compared to average-density UNO-CI and UNO-CAS results. The goal is to establish the extent to which the decomposition in eq 2 affects the performance with respect to results from large active space complete active space self-consistent field (CASSCF) and DMRG calculations. The systems studied are the highly multireference ozone molecule and transition-metalcontaining species nickel-acetylene and ammonia μ -oxo dicopper ammonia (geometries can be found in Tables S1-S4 of the Supporting Information). The cc-PVTZ basis set was used for ozone and nickel-acetylene calculations, and the cc-PVDZ basis set was used for μ -oxo dicopper ammonia calculations. The occupation number thresholds for NO-ASD were 0.02-1.98 and 0.01-1.99 for ozone, 0.02-1.98 for nickel-acetylene, and 0.02-1.98 for μ -oxo dicopper. The code was implemented in a stand-alone in-house code that utilizes the MQCPack library³⁴ as well as interfacing with a modified version of Gaussian 16.35

We first consider the ozone system, in which two stable unrestricted Hartree-Fock (UHF) solutions differing by 0.085 hartree describe the correlation mechanisms within the system (labeled UHF 1 and UHF 2 in Table S5 of the Supporting Information, which shows occupation numbers of NOs of all methods discussed here). Both SCF solutions have two fractionally occupied NOs (occupation numbers between 0.02 and 1.98), although UHF 2 has more diradical character than UHF 1. As a result, the correlation mechanism described in UHF 1 is $n \to \pi^*$, while UHF 2 shows $\sigma \to \pi^*$ character (Figure S1 of the Supporting Information). In contrast, the NOs of large active space CASSCF calculations (12 electrons in 9 orbitals) and DMRG calculations indicate that the fractionally occupied NO space contains 7 and 9 orbitals, respectively. As discussed by Pulay and co-workers, only two of these fractional orbitals lie in the strong correlation regime, while the remaining orbitals have occupation numbers close to the closed shell limit and, therefore, can be considered as intermediately correlated. Occupation numbers from the averaged density of the two SCF solutions indicate four fractionally occupied orbitals, where coupling of the two correlation mechanisms results in doubling of the required active space.

Figure 2 illustrates how the occupation numbers of the different methods examined compare to DMRG, where more

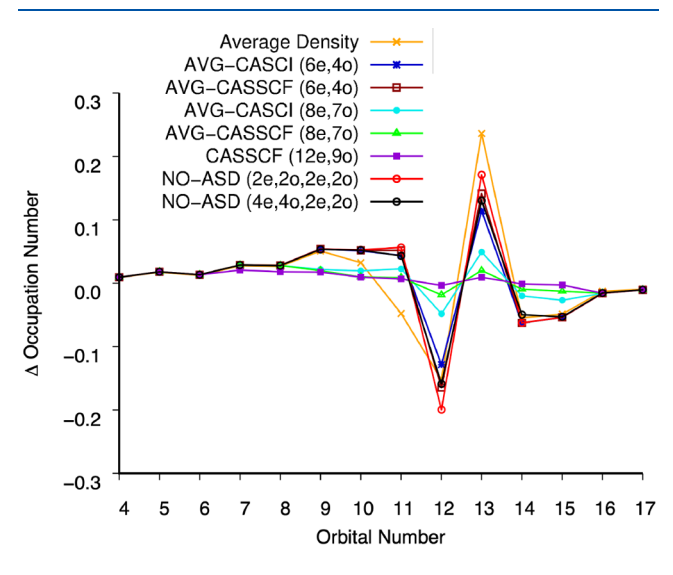


Figure 2. Occupation numbers of valence natural orbitals in ozone compared to a full-valence DMRG for different methods indicated in the legend with the cc-pVTZ basis set.

positive (negative) occupation numbers for low (high) orbital indices indicate a shift toward the closed shell and the highest occupied molecular orbital (HOMO) is index 12, while the lowest unoccupied molecular orbital (LUMO) is index 13. The averaged density NO occupation numbers (orange cross) show that orbitals 10 and 11 are the additional fractionally occupied NOs because their value is similar to or less than the DMRG occupation number. The resulting six electron in four orbital active space can be treated through either using the complete active space configuration interaction (CASCI)⁴ or CASSCF.³ Interestingly, the NO analysis of the CASCI (blue star) and CASSCF (brown open square) densities suggests that there are only three and two orbitals, respectively, in the correlated orbital space. Changing the criteria for fractionally occupied

orbitals to occupation numbers between 0.003 and 1.997 to capture additional intermediate correlation leads to an eight electron in seven orbital active space (CASCI, cyan solid circles; CASSCF, green solid triangles). Including these additional orbitals gives occupation numbers that are much closer to the DMRG and CASSCF using 12 electrons in 9 orbitals (purple solid square), with a seven orbital correlated space. Using the 0.02-1.98 occupation number criteria for the fractionally occupied orbitals leads to a NO-ASD(2e,2o;2e,2o) active space (red open circles), i.e., a two electron in two orbital expansion in the orbitals of UHF 1 and the same in the orbitals of UHF 2. Using occupation number 0.01-1.99 as the criteria leads to NO-ASD(4e,4o;2e,2o), with four orbitals from UHF 1 in the correlated space (black open circles). Both the NO-ASD calculations give NO occupation numbers that are close to the CASCI(6,4) and CASSCF(6,4) results, with NO-ASD(4e,4o;2e,2o) very closely reproducing the CASSCF(6,4)

Table 1 shows how the number of Hamiltonian matrix elements of each method correlates with the correlation energy

Table 1. Number of Hamiltonian Matrix Elements and Error in Correlation Energy with Respect to Full-Valence DMRG Calculation for Different Methods in the Calculation of Ozone Using the cc-pVTZ Basis Set

method	number of Hamiltonian matrix elements	ΔE (kcal mol ⁻¹)
DMRG ^a	6.189×10^{29}	0.0
18e,32o		
CASSCF	4.978×10^7	157.8
12e,9o		
UNO-CASCI ^a	1.501×10^6	194.4
8e,7o (AVG)		
UNO-CASSCF ^a	1.501×10^6	166.2
8e,7o (AVG)		
UNO-CASCI ^a	256	243.8
6e,4o (AVG)		
UNO-CASSCFa	256	241.2
6e,4o (AVG)		
NO-ASD	64	242.4
2e,2o;2e,2o		
NO-ASD	1600	233.6
4e,4o;2e,2o		
an 1	C =	

^aResults were from ref 5.

remaining, assuming that DMRG gives the exact result. Orbital reoptimization of CAS six electron in four orbital active space only reduces the energy by 2.6 kcal mol⁻¹, although with the eight electron in seven orbital active space, the difference was 28.2 kcal mol⁻¹, suggesting that the NOs of intermediate correlated orbitals change their shape to a greater extent than the strongly correlated orbitals. Increasing the active space from six electrons in four orbitals to eight electron in seven orbitals increases the number of matrix elements from 10² to 106, with the correlation energy error decreasing by 49.4 kcal mol⁻¹ for fixed orbitals and 75.0 kcal mol⁻¹ for reoptimized orbitals. Increasing the active space to 12 electrons in 9 orbitals leads to an order of magnitude increase in the number of Hamiltonian matrix elements, while the correlation energy error decreases by only 8.4 kcal mol⁻¹ and remains 157.8 kcal mol⁻¹ above the full-valence active space DMRG calculation. In comparison, the NO-ASD(2e,2o;2e,2o) method with only

64 Hamiltonian matrix elements gives results comparable to CAS(6e,4o), which is has 4 times as many elements. When the stricter criteria for determining fractional occupied orbitals are used, NOASDC(4e,4o;2e,2o) reduces the correlation energy error by 10.2 kcal mol⁻¹, even though the number of matrix elements increases just over 6-fold.

The second system investigated is nickel—acetylene, which was identified by Keller and co-workers as possessing two correlation mechanisms. The two correlation mechanisms in nickel—acetylene are represented by two UHF solutions that differ in energy by just 1.03 kcal mol⁻¹ using the cc-PVTZ basis set (Table S6 of the Supporting Information). The higher energy solution (labeled UHF 1 in Table S6 of the Supporting Information) involves the bonding and antibonding orbital pair consisting of Ni d_{xy} and acetylene π_y^* orbital fragments. The UHF 2 correlation mechanism involves the interaction of orbitals from UHF 1 with the Ni d_z² and Ni 3s orbitals (Figure S2 of the Supporting Information). Figure 3 shows how the

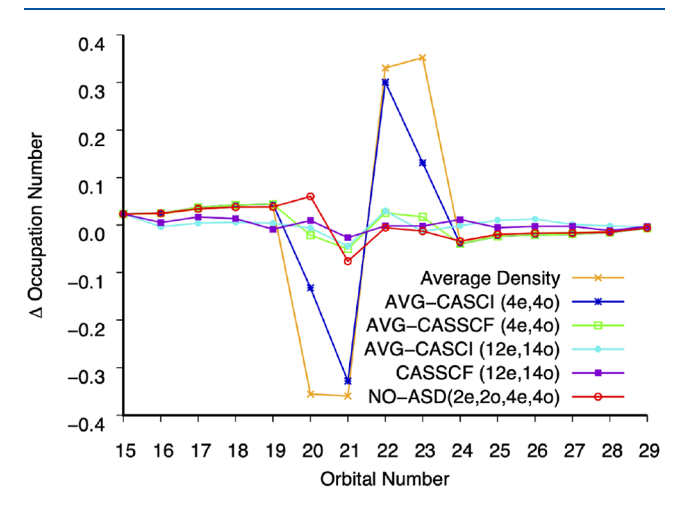


Figure 3. Occupation numbers of valence natural orbitals in nickel—acetylene compared to DMRG(18e,33o) for different methods indicated in the legend with the cc-pVTZ basis set.

occupation numbers of NOs differ from a DMRG(18e,33o) calculation for the methods discussed in the remainder of this paragraph. Orbital 21 is the HOMO orbital index, and orbital 22 is the LUMO orbital index. UHF 1 indicates a two electron in two orbital correlated space, while UHF 2 indicates a four electron in four orbital active space. The NO occupation numbers of the DMRG calculation indicate that a 13 orbital correlated space is required, although all but four of these orbitals are in the intermediately correlated regime. The averaged density from the two UHF solutions (orange crosses) gives NO occupation numbers that suggest a four electron in four orbital correlated space. Performing CASCI(4e,4o) with the strongly correlated NOs of the average density matrix (blue stars) leads to a density matrix with occupation numbers that improve marginally on the UHF averaged density. Reoptimizing the orbitals in a CASSCF(4e,4o) calculation (green open squares) significantly improves the density, giving much closer agreement to DMRG in the occupation numbers of the four strongly correlated NOs, although the intermediately correlated orbitals are not identified and remain closed shell. Capturing the intermediately correlated orbitals requires a 12 electron in 14 orbital calculation, using an occupation number threshold of 0.001-1.999, in which there is no significant difference in the NO occupation numbers, regardless of whether fixed orbitals (cyan solid circles) or reoptimized orbitals (purple solid squares) are used. NO-ASD(2e,2o;4e,4o) suggested by the NO occupation numbers of the UHF solutions (red open circles) gives a significant improvement over the CASCI(4e,4o) calculation, indicating that the additional two electron in two orbital active space in NO-ASD replicates orbital reoptimization in CASSCF(4e,4o) but does not capture intermediate correlated orbitals.

With the analysis of the size of the Hamiltonian with respect to the error in the correlation energy (Table 2), as was done

Table 2. Number of Hamiltonian Matrix Elements and Error in Correlation Energy with Respect to Full-Valence DMRG Calculation for Different Methods in the Calculation of Nickel—Acetylene Using the cc-pVTZ Basis Set

methods	number of Hamiltonian elements	$\Delta E(\text{kcal mol}^{-1})$
DMRG ^a	2.212×10^{30}	0.0
18e,33o		
CASSCF	8.132×10^{13}	35.4
12e,14o		
UNO-CASCI ^a	8.132×10^{13}	96.7
12e,14o (AVG)		
UNO-CASCI ^a	1296	188.3
4e,4o (AVG)		
UNO-CASSCF ^a	1296	185.6
4e,4o (AVG)		
NO-ASD	1600	164.4
2e,2o;4e,4o		
^a Results were from	ref 5.	

above for ozone, it is apparent that the marginal increase in the size of the Hamiltonian of NO-ASD(2e,2o;4e,4o) with respect to CASCI(4e,4o) leads to an order of magnitude improvement in the correlation energy error (-23.9 kcal mol⁻¹) compared to orbital reoptimization with CASSCF(4e,4o) (-2.7 kcal mol⁻¹). To analyze where NO-ASD(2e,2o;4e,4o) lies in the hierarchy of increasing active space size, Table S7 of the Supporting Information shows the energy of averaged density UNO-CASCI with increasing active spaces. It can be seen that the NO-ASD(2e,2o;4e,4o) energy is slightly better than UNO-CASCI(8e,8o), despite comprising significantly fewer determinants. Including all of the intermediate correlated orbitals increases the size of the Hamiltonian by 1010 matrix elements, and without orbital reoptimization still leaves 96.7 kcal mol⁻¹ correlation energy error. The larger improvement in correlation energy upon orbital reoptimization with larger determinant expansions observed in ozone is also observed in nickel-acetylene, reducing the error in correlation energy by 61.3 kcal mol⁻¹, again indicating that the intermediate correlated orbitals are more sensitive to orbital reoptimization than the strongly correlated orbitals.

Lastly, transition metal compounds containing $[Cu_2O_2]^{2+}$ are known to have high catalytic activity with biological relevance. As a result of the variety of ways that copper(I) can bind to oxygen, there are several different possible structures that can exist in biological systems. Previous studies have shown that $[Cu_2O_2]^{2+}$ systems have significant multireference character, and as a result, it is difficult to predict the relative energies of the different structures. Here, we examine the μ -oxo dicopper ammonia complex, and the relative energies of the **bis** and **per** structures (Figure 4). The

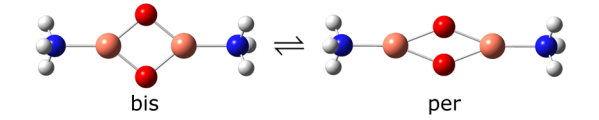


Figure 4. Bis and per isomers of the μ -oxo dicopper ammonia complex.

multireference character of the molecular wave function indicates that large computationally infeasible active spaces are required. The two correlation mechanisms were represented by UHF solutions that were separated by 0.1201 hartree in the **bis** geometry and by 0.1000 hartree in the **per** geometry. The two correlation mechanisms both include copper d_{xy} orbitals interacting with oxygen p_x and p_y orbitals in the first case and with oxygen p_z in the second case (Figures S3 and S4 of the Supporting Information). Natural orbital occupation numbers at the **bis** geometry are shown in Table S8 of the Supporting Information, and natural orbital occupation numbers at the **per** geometry are shown in Table S9 of the Supporting Information.

Examining the average density NOs indicates an eight electron in seven orbital active space at the **bis** geometry, while at the **per** geometry, the indicated active space is six electrons in five orbitals based on a threshold for strongly correlated orbitals of 0.01-1.99 (the NO with occupation number of 0.00998 was also included at the **bis** geometry). The averaged density active spaces lead to Hamiltonian matrices with $10\,000$ matrix elements for (6e,5o) and 1.501×10^6 matrix elements for (8e,7o) (Table 3). For the NO-ASD calculation, a

Table 3. Relative Energies between bis and per Geometries of μ -Oxo Dicopper Ammonia Calculated Using Different Methods with the cc-PVDZ Basis Set, Except the DMRG Calculation Using the ANO-RCC Basis Set

methods	number of Hamiltonian elements	$E(\mathbf{bis}) - E(\mathbf{per})$ $(kcal \ mol^{-1})$
DMRG-CASPT2 ^a	5.347×10^{25}	22.6
24e,24o		
UNO-CASCI ^b	1.501×10^6	-8.9
8e,7o (AVG)		
UNO-CASSCF ^b	1.501×10^6	8.2
8e,7o (AVG)		
UNO-CASCI ^b	10000	-0.1
6e,5o (AVG)		
UNO-CASSCF ^b	10000	9.4
6e,5o (AVG)		
NO-ASD	5184	-3.2
4e,4o;4e,4o		

"Results were taken from ref 40. ^bResults are obtained from the methodology of ref 5.

(4e,4o;4e,4o) active space containing the Hamiltonian matrix containing 5184 matrix elements was used, which is 52% of the smaller (6e,5o) active space and <1% of the larger (8e,7o) active space used with the average density NOs. Despite the smaller size of the NO-ASD Hamiltonian, the absolute energy for the **bis** isomer is energetically lower than that of the average density CASCI(6e,5o) calculation by 7.3 kcal mol⁻¹. One of the strongest demonstrations for the performance of NO-ASD is that the absolute energy for the **per** isomer it is lower than the average density CASCI(6e,5o) and CASCI(8e,7o) calculations by 4.2 and 4.0 kcal mol⁻¹, respectively. Even the

bis CASCI(8e,7o) calculation is only 1.8 kcal mol⁻¹ lower in energy than the NO-ASD(4e,4o;4e,4) calculation, while orbital reoptimization with CASSCF recovers a greater amount of correlation energy by 5.7 and 33.4 kcal mol⁻¹ for the (6e,5o) and (8e,7o) active spaces, respectively. NO occupation numbers of NO-ASD, CASCI, and CASSCF calculations all indicate four strongly correlated orbitals.

With the examination of the difference in energy between the two geometries, NO-ASD gives similar results to the average density CASCI of both size active spaces, in which the per geometry is lower in energy than the bis geometry. DMRG calculations indicate the opposite energy order of bis and per geometries. Allowing for orbital relaxation with CASSCF calculations yields energy ordering consistent with DMRG calculations, suggesting that orbital relaxation is important for properly describing the correct energy order rather than the error in NO-ASD resulting from a breakdown of the correlation mechanism approximation.

In conclusion, we have introduced the concept of the NO-ASD methodology, in which correlation mechanisms are used to partition strong correlation. NO-ASD was then assessed against average density CASCI and CASSCF calculations as well as very large active space DMRG calculations. We demonstrated that NO-ASD gives results consistent with average density CAS expansions, despite the smaller active space, indicating that the partitioning and recouping of strong correlation in the wave function by the correlation mechanism can be used to avoid the computational expense of explicit entanglement of all orbitals. The methodology was assessed in terms of both NO occupation numbers and correlation energy error with respect to DMRG calculations. Especially with larger determinant expansions, orbital reoptimization leads to improvements in the average density CAS calculations. As a result, nonorthogonal orbital reoptimization may provide a route to improve the NO-ASD method.³³ While performing orbital reoptimization on the whole NO-ASD determinant expansion may not be computationally feasible, it is also possible to perform orbital reoptimization through a nonorthogonal multiconfigurational self-consistent field (NOMCSCF) calculation of the underlying SCF solutions that indicates the correlation mechanism. The subsequent reoptimized basis determinants used to partition the wave function and perform NO-ASD expansion are likely to capture a correlation that is absent from the independently optimized SCF solutions.

ASSOCIATED CONTENT

Solution Supporting Information

The Supporting Information is available free of charge at https://pubs.acs.org/doi/10.1021/acs.jpclett.2c03349.

Molecular geometries, total energies, and NO occupation numbers for all systems studied (PDF)

AUTHOR INFORMATION

Corresponding Author

Lee M. Thompson — Department of Chemistry, University of Louisville, Louisville, Kentucky 40205, United States;
ocid.org/0000-0003-1485-5934;

Email: lee.thompson.1@louisville.edu

Authors

- Emily M. Kempfer-Robertson Department of Chemistry, University of Louisville, Louisville, Kentucky 40205, United States
- Andrew D. Mahler Department of Chemistry, University of Louisville, Louisville, Kentucky 40205, United States
- Meagan N. Haase Department of Chemistry, University of Louisville, Louisville, Kentucky 40205, United States
- **Piper Roe** Department of Chemistry, University of Louisville, Louisville, Kentucky 40205, United States

Complete contact information is available at: https://pubs.acs.org/10.1021/acs.jpclett.2c03349

Notes

The authors declare no competing financial interest.

ACKNOWLEDGMENTS

This material is based on work supported by the National Science Foundation under Grant 2144905. Emily M. Kempfer-Robertson acknowledges funding through the Arno Spatola Endowment Fellowship. This work was conducted in part using the resources of the University of Louisville's Research Computing group and the Cardinal Research Cluster. The authors thank Hugh Burton for helpful discussions.

REFERENCES

- (1) Veryazov, V.; Malmqvist, P.; Roos, B. O. How to Select Active Space for Multiconfigurational Quantum Chemistry? *Int. J. Quantum Chem.* **2011**, *111*, 3329–3338.
- (2) Löwdin, P.-O. Quantum Theory of Many-Particle Systems. I. Physical Interpretations by Means of Density Matrices, Natural Spin-Orbitals, and Convergence Problems in the Method of Configurational Interaction. *Phys. Rev.* **1955**, *97*, 1474–1489.
- (3) Bofill, J. M.; Pulay, P. The Unrestricted Natural Orbital-Complete Active Space (UNO-CAS) Method: An Inexpensive Alternative to the Complete Active Space-Self-Consistent-Field (CAS-SCF) Method. J. Chem. Phys. 1989, 90, 3637–3646.
- (4) Pulay, P.; Hamilton, T. P. UHF Natural Orbitals for Defining and Starting MC-SCF Calculations. *J. Chem. Phys.* **1988**, 88, 4926–4933.
- (5) Keller, S.; Boguslawski, K.; Janowski, T.; Reiher, M.; Pulay, P. Selection of Active Spaces for Multiconfigurational Wavefunctions. *J. Chem. Phys.* **2015**, *142*, 244104.
- (6) Parker, S. M.; Seideman, T.; Ratner, M. A.; Shiozaki, T. Communication: Active-Space Decomposition for Molecular Dimers. *J. Chem. Phys.* **2013**, *139*, 021108.
- (7) Mo, Y.; Peyerimhoff, S. D. Theoretical Analysis of Electronic Delocalization. *J. Chem. Phys.* **1998**, *109*, 1687–1697.
- (8) Mo, Y.; Gao, J. An Ab Initio Molecular Orbital–Valence Bond (MOVB) Method for Simulating Chemical Reactions in Solution. *J. Phys. Chem. A* **2000**, *104*, 3012–3020.
- (9) Straatsma, T. P.; Broer, R.; Sánchez-Mansilla, A.; Sousa, C.; de Graaf, C. GronOR: Scalable and Accelerated Nonorthogonal Configuration Interaction for Molecular Fragment Wave Functions. *J. Chem. Theory Comput.* **2022**, *18*, 3549–3565.
- (10) Wu, Q.; Cheng, C.-L.; van Voorhis, T. Configuration Interaction Based on Constrained Density Functional Theory: A Multireference Method. *J. Chem. Phys.* **2007**, *127*, 164119–10.
- (11) Thouless, D. J. Stability Conditions and Nuclear Rotations in the Hartree-Fock Theory. *Nucl. Phys.* **1960**, *21*, 225–232.
- (12) Chan, G. K. Low Entanglement Wavefunctions. Wiley Interdiscip. Rev.: Comput. Mol. Sci. 2012, 2, 907–920.
- (13) Lu, Y.; Zhao, R.; Zhang, J.; Liu, M.; Gao, J. Minimal Active Space: NOSCF and NOSI in Multistate Density Functional Theory. *J. Chem. Theory Comput.* **2022**, *18*, 6407–6420.

- (14) Lu, Y.; Gao, J. Fundamental Variable and Density Representation in Multistate DFT for Excited States. *J. Chem. Theory Comput.* **2022**, *18*, 7403–7411.
- (15) Lu, Y.; Gao, J. Multistate Density Functional Theory of Excited States. J. Phys. Chem. Lett. 2022, 13, 7762–7769.
- (16) Burton, H. G. A.; Wales, D. J. Energy Landscapes for Electronic Structure. *J. Chem. Theory Comput.* **2021**, *17*, 151–169.
- (17) Burton, H. G. A. Energy Landscape of State-Specific Electronic Structure Theory. J. Chem. Theory Comput. 2022, 18, 1512–1526.
- (18) Gilbert, A. T. B.; Besley, N. A.; Gill, P. M. W. Self-Consistent Field Calculations of Excited States Using the Maximum Overlap Method (MOM). *J. Phys. Chem. A* **2008**, *112*, 13164–13171.
- (19) Thom, A. J. W.; Head-Gordon, M. Locating Multiple Self-Consistent Field Solutions: An Approach Inspired by Metadynamics. *Phys. Rev. Lett.* **2008**, *101*, 193001–4.
- (20) Tóth, Z.; Pulay, P. Finding Symmetry Breaking Hartree-Fock Solutions: The Case of Triplet Instability. *J. Chem. Phys.* **2016**, *145*, 164102.
- (21) Barca, G. M. J.; Gilbert, A. T. B.; Gill, P. M. W. Simple Models for Difficult Electronic Excitations. *J. Chem. Theory Comput.* **2018**, *14*, 1501–1509.
- (22) Thompson, L. M. Global Elucidation of Broken Symmetry Solutions to the Independent Particle Model through a Lie Algebraic Approach. *J. Chem. Phys.* **2018**, *149*, 194106.
- (23) Dong, X.; Mahler, A. D.; Kempfer-Robertson, E. M.; Thompson, L. M. Global Elucidation of Self-Consistent Field Solution Space Using Basin Hopping. *J. Chem. Theory Comput.* **2020**, *16*, 5635–5644.
- (24) Carter-Fenk, K.; Herbert, J. M. State-Targeted Energy Projection: A Simple and Robust Approach to Orbital Relaxation of Non-Aufbau Self-Consistent Field Solutions. *J. Chem. Theory Comput.* **2020**, *16*, 5067–5082.
- (25) Mayer, I.Simple Theorems, Proofs, and Derivations in Quantum Chemistry; Springer: New York, 2003; DOI: 10.1007/978-1-4757-6519-9.
- (26) Thom, A. J. W.; Head-Gordon, M. Hartree-Fock Solutions as a Quasidiabatic Basis for Nonorthogonal Configuration Interaction. *J. Chem. Phys.* **2009**, *131*, 124113.
- (27) Burton, H. G. A. Generalized Nonorthogonal Matrix Elements: Unifying Wick's Theorem and the Slater-Condon Rules. *J. Chem. Phys.* **2021**, *154*, 144109.
- (28) Burton, H. G. A. Generalized Nonorthogonal Matrix Elements for Arbitrary Excitations. arXiv.org, e-Print Arch., Phys. 2022, arXiv:2208.10208 (accessed Oct 16, 2022).
- (29) Sanchez de Meras, A.; Lepetit, M.-B.; Malrieu, J.-P. Discontinuity of valence CASSCF wave functions around weakly avoided crossing between valence configurations. *Chem. Phys. Lett.* **1990**, *172*, 163–168.
- (30) Bone, R. G. A.; Pulay, P. Half-Projected Hartree-Fock Natural Orbitals for Defining CAS-SCF Active Spaces. *Int. J. Quantum Chem.* **1993**, 45, 133–166.
- (31) Burton, H. G. A.; Thom, A. J. W. Holomorphic Hartree-Fock Theory: An Inherently Multireference Approach. *J. Chem. Theory Comput.* **2016**, *12*, 167–173.
- (32) Burton, H. G. A.; Gross, M.; Thom, A. J. W. Holomorphic Hartree-Fock Theory: The Nature of Two-Electron Problems. *J. Chem. Theory Comput.* **2018**, *14*, 607–618.
- (33) Mahler, A. D.; Thompson, L. M. Orbital Optimization in Nonorthogonal Multiconfigurational Self-Consistent Field Applied to the Study of Conical Intersections and Avoided Crossings. *J. Chem. Phys.* **2021**, *154*, 244101.
- (34) Thompson, L. M.; Sheng, X.; Mahler, A.; Mullally, D.; Hratchian, H. P.MQCPack 22.6. *Zenodo*; European Organization for Nuclear Research (CERN): Geneva, Switzerland, 2022; DOI: 10.5281/zenodo.6644196.
- (35) Frisch, M. J.; Trucks, G. W.; Schlegel, H. B.; Scuseria, G. E.; Robb, M. A.; Cheeseman, J. R.; Scalmani, G.; Barone, V.; Petersson, G. A.; Nakatsuji, H.; Li, X.; Caricato, M.; Marenich, A. V.; Bloino, J.; Janesko, B. G.; Gomperts, R.; Mennucci, B.; Hratchian, H. P.; Ortiz, J.

- V.; Izmaylov, A. F.; Sonnenberg, J. L.; Williams-Young, D.; Ding, F.; Lipparini, F.; Egidi, F.; Goings, J.; Peng, B.; Petrone, A.; Henderson, T.; Ranasinghe, D.; Zakrzewski, V. G.; Gao, J.; Rega, N.; Zheng, G.; Liang, W.; Hada, M.; Ehara, M.; Toyota, K.; Fukuda, R.; Hasegawa, J.; Ishida, M.; Nakajima, T.; Honda, Y.; Kitao, O.; Nakai, H.; Vreven, T.; Throssell, K.; Montgomery, J. A., Jr.; Peralta, J. E.; Ogliaro, F.; Bearpark, M. J.; Heyd, J. J.; Brothers, E. N.; Kudin, K. N.; Staroverov, V. N.; Keith, T. A.; Kobayashi, R.; Normand, J.; Raghavachari, K.; Rendell, A. P.; Burant, J. C.; Iyengar, S. S.; Tomasi, J.; Cossi, M.; Millam, J. M.; Klene, M.; Adamo, C.; Cammi, R.; Ochterski, J. W.; Martin, R. L.; Morokuma, K.; Farkas, O.; Foresman, J. B.; Fox, D. J. Gaussian 16, Revision A.03; Gaussian, Inc.: Wallingford, CT, 2016.
- (36) Que, L., Jr.; Tolman, W. B. Bis(μ-oxo)dimetal "Diamond" Cores in Copper and Iron Complexes Relevant to Biocatalysis. *Angew. Chem., Int. Ed.* **2002**, *41*, 1114–1137.
- (37) Cramer, C. J.; Włoch, M.; Piecuch, P.; Puzzarini, C.; Gagliardi, L. Theoretical Models on the Cu_2O_2 Torture Track: Mechanistic Implications for Oxytyrosinase and Small-Molecule Analogues. *J. Phys. Chem. A* **2006**, *110*, 1991–2004.
- (38) Gherman, B. F.; Cramer, C. J. Quantum Chemical Studies of Molecules Incorporating a $\text{Cu}_2\text{O}_2^{2+}$ Core. Coord. Chem. Rev. 2009, 253, 723–753.
- (39) Liakos, D. G.; Neese, F. Interplay of Correlation and Relativistic Effects in Correlated Calculations on Transition-Metal Complexes: The $(Cu_2O_2)^{2+}$ Core Revisited. *J. Chem. Theory Comput.* **2011**, 7, 1511–1523.
- (40) Wang, Q.; Zou, J.; Xu, E.; Pulay, P.; Li, S. Automatic Construction of the Initial Orbitals for Efficient Generalized Valence Bond Calculations of Large Systems. *J. Chem. Theory Comput.* **2019**, 15, 141–153.